

Accepted for publication in the Astrophysical Journal

## Cool Companions to White Dwarfs from the 2MASS Second Incremental Data Release

Stefanie Wachter

*SIRTF Science Center, California Institute of Technology, MS 220-6, Pasadena, CA 91125*

wachter@ipac.caltech.edu

D. W. Hoard

*SIRTF Science Center, California Institute of Technology, MS 220-6, Pasadena, CA 91125*

hoard@ipac.caltech.edu

and

Kathryn H. Hansen, Rebecca E. Wilcox, Hilda M. Taylor, Steven L. Finkelstein

*University of Washington, Department of Astronomy, Box 351580, Seattle, WA 98195*

### ABSTRACT

We present near-infrared magnitudes for all white dwarfs (selected from the catalog of McCook & Sion) contained in the 2 Micron All Sky Survey Second Incremental Data Release. We show that the near-IR color-color diagram is an effective means of identifying candidate binary stars containing a WD and a low mass main sequence star. The loci of single WDs and WD + red dwarf binaries occupy distinct regions of the near-IR color-color diagram. We recovered all known unresolved WD + red dwarf binaries located in the 2IDR sky coverage, and also identified as many new candidate binaries (47 new candidates out of 95 total). Using observational near-IR data for WDs and M–L dwarfs, we have compared a sample of simulated WD + red dwarf binaries with our 2MASS data. The colors of the simulated binaries are dominated by the low mass companion through the late-M to early-L spectral types. As the spectral type of the companion becomes progressively later, however, the colors of unresolved binaries become progressively bluer. Binaries containing the lowest mass companions will be difficult to distinguish from single WDs solely on the basis of their near-IR colors.

*Subject headings:* Binaries: general — infrared: stars — stars: fundamental parameters, surveys — white dwarfs

arXiv:astro-ph/0212174v1 6 Dec 2002

## 1. Introduction

In the search for extrasolar planets, various methods have been employed to detect the signatures of faint stellar and sub-stellar companions. For main sequence primary stars, faint low mass companions are often hidden in the glare of the more luminous primary, and radial velocity variations are small and therefore difficult to detect. On the other hand, observing low mass companions to white dwarfs (WDs) offers many advantages compared to main sequence primaries. Since WDs are less luminous than main sequence stars, the brightness contrast compared to a potential faint companion is significantly reduced. Most importantly, the markedly different spectral energy distributions of the WDs and their low mass companions makes the detection and separation of the two components relatively straightforward even with simple broad-band multi-color photometry.

Because WDs have traditionally been identified and studied via observations in the blue part of the spectrum, comparatively little is known about their infrared (IR) properties. The recent discovery that very cool WDs are much bluer in the IR than previously thought to be the case (Hodgkin et al. 2000) highlights how little is known about WD spectral properties at longer wavelengths. Consequently, we are studying the group near-IR photometric properties of WDs. In this paper, we present analysis of the near-IR color-color diagram of WDs, which demonstrates a means of identifying candidates for WDs with close (unresolved), cool, low mass stellar or sub-stellar companions.

## 2. Target Selection and Identification

We selected the WDs in our sample from the catalog of spectroscopically identified WDs by McCook & Sion (1999, hereafter, MS99). We extracted all WDs from MS99 that are contained in the sky coverage of the 2MASS Second Incremental Data Release (2IDR; e.g., Skrutskie et al. 1995, 1997)<sup>1</sup>. Due to potentially large and often unknown proper motions, and other uncertainties in published positions, we first identified each WD in optical images from the Digitized Sky Survey (DSS). The WD in the optical image was then matched with sources in the 2MASS 2IDR images and point source catalog. Our identification of the optical counterpart was based on published finding charts whenever possible; for example, using the charts in the LHS atlas (Luyten & Albers 1979), the Giclas proper motion survey and lists of suspected WDs (e.g., Giclas 1958 through Giclas, Burnham, & Thomas 1980), and the Montreal-Cambridge-Tololo survey (Lamontagne et al. 2000), to name only a few

---

<sup>1</sup>Also see <http://pegasus.phast.umass.edu/>.

sources. The WDs for which no finding chart could be located in the literature were identified from a combination of published coordinates, proper motion, and color in the DSS images. A catalog detailing accurate J2000 positions together with references to individual finding charts and our method(s) of identification will be presented in a future paper.

## 2.1. Number Statistics

MS99 list 2249 spectroscopically identified WDs, 1235 of which are located in the sky coverage of the 2MASS 2IDR. For 47 WDs, we could not (re)establish an optical identification. This was mainly due to insufficient accuracy in the published finding charts and/or coordinates that made it impossible to decide with confidence between several stars close to the given positions. In some cases, WDs listed in MS99 have subsequently been reclassified as AGN, Seyfert galaxies, or hot subdwarfs. A few WDs appear in MS99 multiple times under different designations. For 27 WDs, no IR magnitudes could be obtained from the 2MASS 2IDR point source catalog despite having an identified optical counterpart. In the majority of cases, this is due to blending of the WD with unrelated field stars in the 2MASS images. Detailed comments on particularly problematic identifications will be provided in a future paper.

The 2MASS completeness limits (defined by photometry with signal-to-noise of  $S/N > 10$ ) are  $J = 15.8$ ,  $H = 15.1$ , and  $K_s = 14.3$ . The survey detection limits are approximately one magnitude fainter in each band. Of the 1161 WDs for which we could establish secure identifications, 759 are detected in the 2MASS 2IDR with varying degrees of accuracy. The remaining 402 WDs are undetected, meaning that while we have securely identified an IR counterpart for these WDs, there is no corresponding entry in the 2MASS 2IDR point source catalog. Many of the formally undetected WDs appear to lie just below the detection limits of the survey, as faint objects are often visible in the 2MASS images at the correct positions.

## 3. Analysis and Discussion

### 3.1. The IR Color-Color Diagram

Figure 1 illustrates the results of our study as a near-IR color-color diagram of WDs. We have plotted all WDs detected in the 2MASS 2IDR, together with the fiducial tracks of the main sequence and the region occupied by L dwarfs. The positions of the spectral type labels are offset horizontally for A0–K5, and vertically for M0–M8. The main sequence data up to M5 were taken from Bessell & Brett (1988) and transformed to the 2MASS photometric

system using the relations in Carpenter (2001), while the colors for late-M and L dwarfs represent mean 2MASS observational data from Gizis et al. (2000) and Kirkpatrick et al. (2000). The points are symbol-coded according to the  $1\text{-}\sigma$  uncertainties of the original IR magnitudes: large filled circles =  $\sigma < 0.1$  mag for  $J$ ,  $H$ , and  $K_s$ ; small filled circles =  $\sigma > 0.1$  mag for at least one of  $J$ ,  $H$ , or  $K_s$ ; small unfilled circles = at least one magnitude is close to the 2MASS faint detection limit and lacks a formal uncertainty.

If we examine only the data points with the smallest uncertainties (large filled circles), then our color-color diagram exhibits two prominent concentrations of points. One group is clustered around the main sequence track of early spectral types to about K0, and another group is clustered around the locus of main sequence M stars. We expect that the former group contains isolated WDs and the WD components of wide (resolved<sup>2</sup>) binaries. The latter group contains close (unresolved) binaries consisting of a WD and a low mass main sequence companion, in which the red spectral energy distribution of the companion dominates the overall color.

In Figure 2, we show the near-IR color-color diagram of 152 *single*, cool WDs (large black circles) from the study of Bergeron et al. (2001). The data have been transformed from the CIT to the 2MASS photometric system using the relations in Carpenter (2001). Typical photometric uncertainties in the transformed Bergeron data are about 5%, with a few objects having larger uncertainties on the order of 10%. It is clear from the Bergeron data that single WDs populate the near-IR color-color diagram close to the locus of A–G main sequence stars, corresponding to the first cluster of points in our 2MASS color-color diagram. Unresolved double degenerate (WD + WD) binaries would, of course, also be located in this region and cannot be distinguished from single WDs in the color-color diagram. In comparison to the Bergeron sample, our data (limited to the sub-set with photometric uncertainties of  $\sigma_{\text{JHK}} < 0.1$  mag) cover a somewhat larger range in color space. This is partially due to the fact that the Bergeron sample was selected to include only cool ( $T_{\text{eff}} \lesssim 12,000$  K) WDs with known parallaxes, while our sample contains a significant number of hotter WDs. We performed a literature search that yielded temperatures for 114 WDs in our low-uncertainty sub-set, 55 of which have  $T_{\text{eff}} > 12,000$  K. Those hot WDs generally populate the blue (lower left) corner of the color-color diagram around (and below) the locus of the main sequence A stars. Further differences between the color distributions of the two data sets are due to the lack of an exact 1:1 match of the particular WDs contained in each sample (that is, due to individual color differences from one WD to another), combined with the uncertainties

---

<sup>2</sup>During our study, we found that, in general, binaries with separations of  $d \leq 2''$  are unresolved in the 2MASS images, while those with separations of  $d \geq 4''$  are resolved. We assessed known binaries with separations of  $2'' < d < 4''$  on a case-by-case basis.

in the photometry. Even a relatively small uncertainty of  $\lesssim \pm 0.1$  mag in each color allows for a substantial shift in the placement of an individual object in the color-color diagram. The 206 WDs with the smallest uncertainties in our data set (large filled circles in Figure 1) have mean uncertainties of  $\langle \sigma_{H-K_s} \rangle = \pm 0.07$  mag and  $\langle \sigma_{J-H} \rangle = \pm 0.06$  mag, while those in the Bergeron sample are on the order of  $\pm 0.07$  mag in each color index.

As mentioned above, we identify the clustering around the M star fiducial track in Figure 1 as unresolved binary systems containing a WD and a low mass main sequence companion. The gap between the two data clusters in Figure 1 (coincident with the locus of K0–K5 main sequence stars) can be attributed to several factors. As indicated by the Bergeron sample, we do not expect single WDs in this color region. Consequently, only a binary consisting of a WD and a K dwarf companion would be located in this area of the color-color diagram. Such composite systems are difficult to identify since the K star overwhelms the combined spectrum at optical–near-IR wavelengths. Furthermore, such systems are intrinsically rare simply due to a mass function effect; that is, if the binaries formed from a random pairing of stars from the same initial mass function, then there are, in general, fewer K stars than M stars as potential companions. Assuming a standard initial mass function (Kroupa 2002), we calculate 0.079 for the expected ratio of K0–K5 to M0–M5 stars. This can be compared to the number of objects in the color bins corresponding to those spectral types in our data sample, for which we derive a ratio of  $\approx 0.07$ . However, we caution that the photometric uncertainties make it unclear whether some of the systems belong to the M or K spectral type bins. A change in the spectral type classification of these systems could alter the value of this ratio, between extreme cases of  $\approx 0.06$ – $0.20$ .

Based on a comparison with the location of single WDs in the color-color diagram (from Figure 2), we selected all objects with  $(J - H) > 0.4$  mag as WD + low mass main sequence star binary candidates. After eliminating objects with the highest photometric uncertainties (small unfilled circles), we find 95 such binary star candidates. Thirty-nine (41%) of these candidates are already listed as binaries in MS99. However, the references to their binary status contained in MS99 reveal that four of these are wide (resolved) binaries, whereas our 2MASS photometry suggests that the WD component may also be an unresolved WD + red dwarf<sup>3</sup> pair. We were unable to locate published information about the separations of another five of the known binaries. We also performed a literature search with SIMBAD for each of our candidates, which identified 13 additional known binaries that are not classified as such in MS99. Table 1 lists all of our candidates together with notes and references regarding their binary classification status. Altogether, approximately half (47 out of 95) of

---

<sup>3</sup>Throughout this paper we will refer to both M and L type main sequence stars as “red dwarfs.”

our candidates are previously *unknown* to be binaries.

Because of the limited spatial resolution of 2MASS ( $2'' \text{ pixel}^{-1}$ ), we investigated whether a chance superposition of a red field star could have produced a significant number of our binary candidates. However, visual inspection of the optical (DSS) and IR images shows that none of our candidates are located in crowded fields, so that the likelihood of a chance superposition is very small. There are 50 additional objects classified as binaries in MS99 that are detected in the 2MASS 2IDR, but were *not* selected by our color criterion as unresolved binary candidates. Forty-two of those are known to be resolved binaries, in which we can separately detect the WD and red dwarf components. Four are unresolved double degenerate (WD + WD) binaries, which are indistinguishable from single WDs in the color-color diagram. The remaining four are unresolved WD + main sequence binaries in which the companion has spectral type earlier than K (hence, these systems are dominated by the bright companion and fall along the main sequence in the color-color diagram, intermingled with the single WDs and below our color selection criterion). Thus, our 2MASS data allows us to recover *all* of the known, unresolved WD + red dwarf binaries from MS99 that are detected in the 2MASS 2IDR.

### 3.2. Simulated Binary Colors

While the red colors of the low mass companions provide a striking contrast to those of the WDs, the luminosity of the low mass stars also rapidly declines as the companion mass decreases. In order to properly evaluate the relative contribution of the WD and the red companion to the overall color of a binary, we calculated the expected colors from random pairings of a WD and a M–L dwarf. We combined (as fluxes) the  $JHK_s$  magnitudes of the sub-set of Bergeron WDs with known distances (and, hence, absolute magnitudes) with the absolute  $JHK_s$  magnitudes of M–L stars (Hawley et al. 2002) to produce a set of simulated binary colors. The resulting simulated binaries are shown as small grey circles in Figure 2. Recall that the large black circles in this figure represent the original single WD data from Bergeron et al. (2001). The solid black line is a schematic track demonstrating the effect on the combined color as a given WD is successively combined with later and later spectral type stars. In general, after a short excursion into the region occupied by early-L dwarfs, the red companion becomes too faint to dominate the combined colors of the system. For progressively later L type companions, the binary color moves blueward, back towards the locus of single WDs.

It is apparent from this simulation that some systems with colors close to those of single WDs may actually contain low mass L dwarf companions. Consequently, we selected a second

group of WDs from our 2MASS data set that satisfy the color criteria  $0.2 \leq (H - K_s) \leq 0.5$  and  $0.1 \leq (J - H) \leq 0.4$ . These 15 objects are listed as tentative binary candidates in Table 2. Four of them are identified as known binaries by MS99. Interestingly, however, all of these are classified as wide (resolved) binaries, which may imply that they are really triple systems, in which the WD component is actually an unresolved WD + red dwarf binary as well. Another one of them (WD0710+741) is a known close (unresolved) binary. Marsh & Duck (1996) used radial velocity data to estimate the mass of the WD’s companion as  $0.08\text{--}0.10M_\odot$ , which is consistent with a late-M to early-L spectral type.

### 3.3. Comparison to Previous Studies

Previous dedicated searches for cool companions to WDs using near-IR observations have been conducted by Probst (1983, henceforth, P83), Zuckerman & Becklin (1992), and Green, Ali, & Napiwotzki (2000, henceforth, GAN00). P83 surveyed 113 relatively bright WDs in  $K$  with a  $12''$ -aperture, single-pixel InSb detector. This survey was somewhat hampered by the lack of spatial resolution and because the majority of WDs were observed in only the  $K$  filter (only 28 of the P83 targets have measurements in all three bands,  $JHK$ ). The presence of IR excess (indicating a possible cool companion) was deduced by comparison of the observed  $K$  magnitude with that predicted by model calculations. Out of the 113 objects surveyed, only seven objects exhibited IR excess and could be readily deconvolved into a WD + red dwarf pair. Six additional objects are identified as “anomalous composites,” which showed moderate IR excess but could not be separated into a WD + red dwarf pair via model fits. Our  $K_s$  band measurements agree well with those of P83 for almost all of the 49 targets in common between our studies. Four of the binary candidates identified by P83 are located in the 2MASS 2IDR sky coverage. Three of these four (0034–211, 0429+176, and 1333+487) are listed in MS99 as binaries and are also found as binary candidates in our 2MASS data. The fourth object, WD 1919+145, is listed in P83 as an “anomalous composite” with moderate IR excess; however, its 2MASS colors in our data place it in the locus of single WDs.

Zuckerman & Becklin (1992) expanded the survey by P83 to include  $\sim 200$  WDs. They found likely cool companions within  $6''$  of 21 WDs. They do not provide their entire list of surveyed WDs (only the binary candidates), so we cannot perform a full comparison to our data. Eight of their binary candidates overlap with our 2MASS sample and six of these (0710+741, 0752–146, 1026+002, 1123+189, 1210+464, and 2256+249) are also identified as binary candidates in our data. The remaining two are a resolved binary and an unresolved double degenerate.

Finally, GAN00 obtained  $J$  and  $K$  band observations of 49 *Extreme Ultraviolet Explorer*-selected hot WDs. Ten of these WDs exhibit significant IR excess, five of which were previously known to be WD + red dwarf binaries. Thirty-four of the 49 WDs from GAN00 are located in the 2MASS 2IDR sky coverage, but six of these are too faint and were not detected (another, WD0427+741J, was one of the ten found to have an IR excess, but it is near the faint detection limit for 2MASS, lacks formal photometric uncertainties, and is not included in our list of binary candidates). Of the remaining 27 objects that were detected by 2MASS, three are known unresolved binaries listed in MS99 (0148–255J, 1123+189 and 1631+781), while two more were identified as binaries in other literature sources (0131–163 and 1711+667J) – see Table 1. (These are the same five objects noted by GAN00 as previously known binaries.)

#### 4. Conclusions

We have shown that the near-IR color-color diagram is an effective means of identifying candidate binary stars containing a WD and a low mass main sequence star. The loci of single WDs and WD + red dwarf binaries occupy distinct regions of the near-IR color-color diagram. Using our data from the 2MASS 2IDR, we recovered all known unresolved WD + red dwarf binaries located in the 2IDR sky coverage, and also identified nearly as many new candidate binaries (47 new candidates out of 95 total). In addition, a handful of the known resolved binaries may actually be triple systems, in which the WD component is itself an unresolved WD + red dwarf binary. We expect to be able to more than double again the number of candidate binaries using the forthcoming full sky data release from 2MASS.

Using observational near-IR data for WDs and M–L dwarfs, we have compared a sample of simulated WD + red dwarf binaries with our 2MASS data. The colors of the simulated binaries are dominated by the low mass companion through the late-M to early-L spectral types. As the spectral type of the companion becomes progressively later, however, the colors of unresolved binaries become progressively bluer. Binaries containing the lowest mass companions will be difficult to distinguish from the locus of single WDs in the near-IR color-color diagram. We have identified an additional 15 WDs that may comprise such binaries. It is encouraging that one of these has been found to be a close WD + red dwarf binary in which the companion has a mass of  $\lesssim 0.1M_{\odot}$  (Marsh & Duck 1996). In order to distinguish the WD + red dwarf binaries from single WDs for systems containing the lowest mass L dwarfs (and brown dwarfs), it is likely to be necessary to observe further into the infrared; for example, at the mid-IR wavelengths observable with the *Space Infrared Telescope Facility* (e.g., Igance 2002).



We thank Roc Cutri (for a helpful discussion about the 2MASS colors of main sequence stars), Gus Muench-Nasrallah (for sharing his insight into initial mass functions), and Vandana Desai and Oliver Fraser (who helped locate WDs in 2MASS images in exchange for pizza). R.E.W. thanks the DeEtte McAuslan Stuart Scholarship Committee, the Boeing Company, and the National Merit Scholarship Corporation for their financial support. The research described in this paper was carried out, in part, at the Jet Propulsion Laboratory, California Institute of Technology, and was sponsored by the National Aeronautics and Space Administration. This publication makes use of data products from the 2 Micron All Sky Survey, which is a joint project of the University of Massachusetts and the Infrared Processing and Analysis Center/California Institute of Technology, funded by the National Aeronautics and Space Administration and the National Science Foundation. It also utilized NASA's Astrophysics Data System Abstract Service and the SIMBAD database operated by CDS, Strasbourg, France, as well as images from the Digitized Sky Survey, which was produced at the Space Telescope Science Institute under US Government grant NAG W-2166. (The images of these surveys are based on photographic data obtained using the Oschin Schmidt Telescope on Palomar Mountain and the UK Schmidt Telescope. The plates were processed into the present compressed digital form with the permission of these institutions.)

## REFERENCES

- Allard, F., Wesemael, F., Fontaine, G., Bergeron, P., Lamontagne, R. 1994, *AJ*, 107, 1565
- Bessell, M. S., Brett, J. M. 1988, *PASP*, 100, 1134
- Bergeron, P., Leggett, S. K., Ruiz, M. T. 2001, *ApJS*, 133, 413
- Bragaglia, A., Greggio, L., Renzini, A., D’Odorico, S. 1990, *ApJ*, 365, L13
- Carpenter, J. M. 2001, *AJ*, 121, 2851
- Finley, D. S., Koester, D., Basri, G. 1997, *ApJ*, 488, 375
- Fulbright, M. S., Liebert, J. 1993, *ApJ*, 410, 275
- Giclas, H. L. 1958, *Lowell Observatory Bulletin*, 4, 1
- Giclas, H. L., Burnham, R., Thomas, N. G. 1980, *Lowell Observatory Bulletin*, 8, 157
- Gizis, J. E., Monet, D. G., Reid, I. N., Kirkpatrick, J. D., Liebert, J., Williams, R. J. 2000, *AJ*, 120, 1085
- Gizis, J. E., Reid, I. N. 1997, *PASP*, 109, 849
- Green, P. J., Ali, B., Napiwotzki, R. 2000, *ApJ*, 540, 992 (GAN00)
- Greenstein, J. L. 1986, *AJ*, 92, 867
- Hawley, S. L., et al. 2002, *AJ*, 123, 3409
- Hodgkin, S. T., Oppenheimer, B. R., Hambly, N. C., Jameson, R. F., Smartt, S. J., Steele, I. A. 2000, *Nature*, 403, 57
- Ignace, R. 2002, *PASP*, 113, 1227
- Kirkpatrick, J. D., et al. 2000, *AJ*, 120, 447
- Koester, D., et al. 2001, *A&A*, 378, 556
- Kroupa, P. 2002, *Science*, 295, 82
- Lamontagne, R., Demers, S., Wesemael, F., Fontaine, G., Irwin, M. J. 2000, *AJ*, 119, 241
- Liebert, J., Schmidt, G. D., Lesser, M., Stepanian, J. A., Lipovetsky, V. A., Chaffe, F. H., Foltz, C. B., Bergeron, P. 1994, *ApJ*, 421, 733

- Luyten, W. J., Albers, H. 1979, LHS Atlas (Minneapolis: University of Minnesota)
- Marsh, T. R., Duck, S. R. 1996, MNRAS, 278, 565
- McCook, G. P., Sion, E. M. 1999, ApJS, 121, 1 (MS99)
- Orosz, J. A., Wade, R. A., Harlow, J. J. B., Thorstensen, J. R., Taylor, C. J., Eracleous, M. 1999, AJ, 117, 1598
- Probst, R. G. 1983, ApJS, 53, 335 (P83)
- Reid, I. N. 1996, AJ, 111, 2000
- Reid, N., Wegner, G., Wickramasinghe, D. T., Bessell, M. S. 1988, AJ, 96, 275
- Schultz, G., Zuckerman, B., Becklin, E. E., Barnbaum, C. 1993, BAAS, 25, 824
- Schultz, G., Zuckerman, B., Becklin, E. E. 1996, ApJ, 460, 402
- Sion, E. M., Oswalt, T. D., Liebert, J., Hintzen, P. 1991, AJ, 101, 1476
- Skrutskie, M. F., et al. 1995, AAS, 187, 75.07
- Skrutskie, M. F., et al. 1997, in The Impact of Large Scale Near-IR Sky Surveys, eds. F. Garzon, et al. (Dordrecht: Kluwer Academic Publishing Company), 25
- Stepanian, J. A., Green, R. F., Foltz, C. B., Chaffee, F., Chavushyan, V. H., Lipovetsky, V. A., Erastova, L. K. 2001, AJ, 122, 3361
- Zuckerman, B., Becklin, E. E. 1992, ApJ, 386, 260

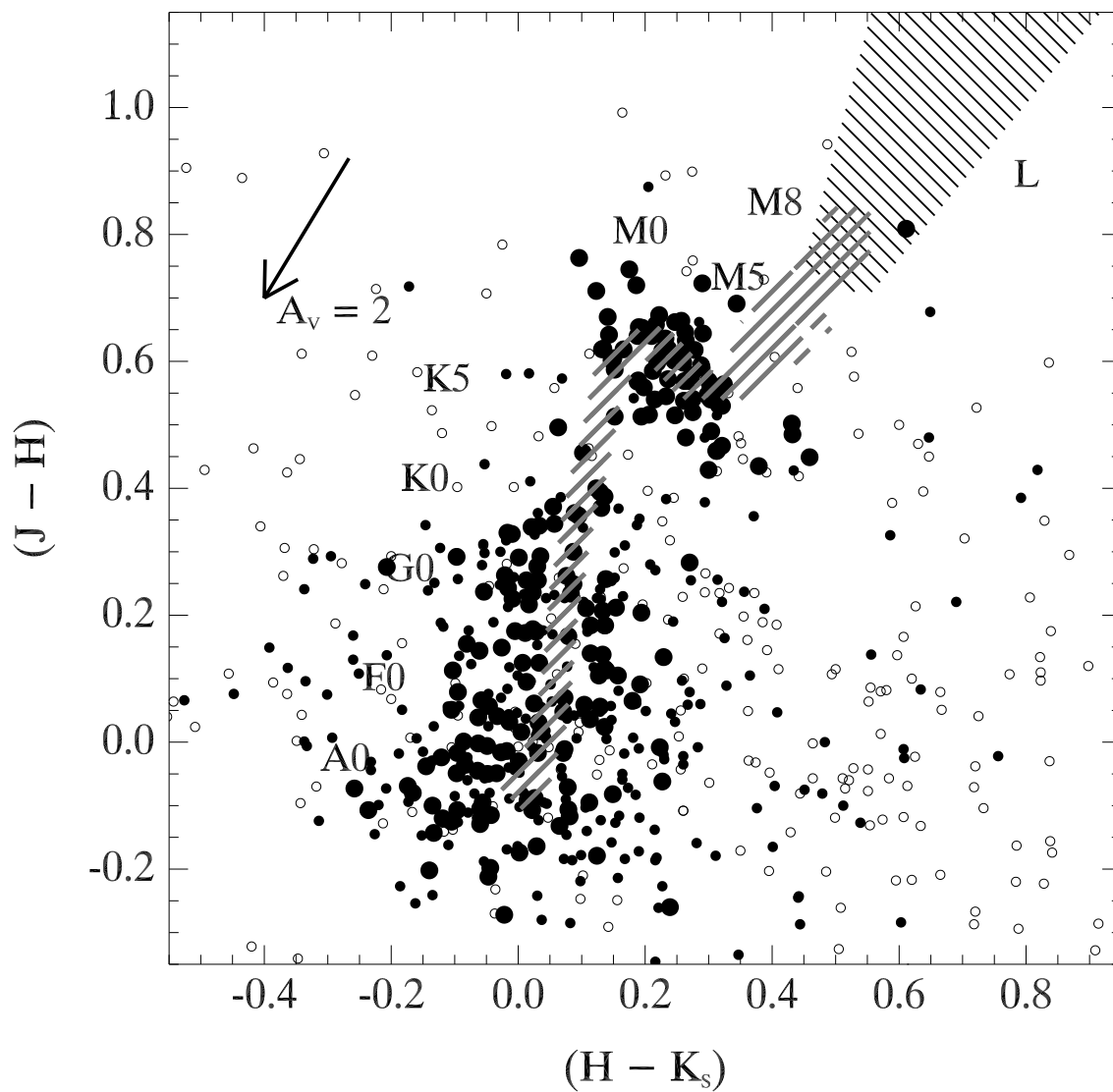


Fig. 1.— Near-IR color-color diagram for WDs from MS99 that are detected in the 2MASS 2IDR. Also shown are the fiducial tracks for the main sequence (/// cross-hatches) and the region occupied by L dwarfs (\\ \\ cross-hatches). The points are symbol-coded according to the  $1\sigma$  uncertainties of the photometry (see section 3.1).

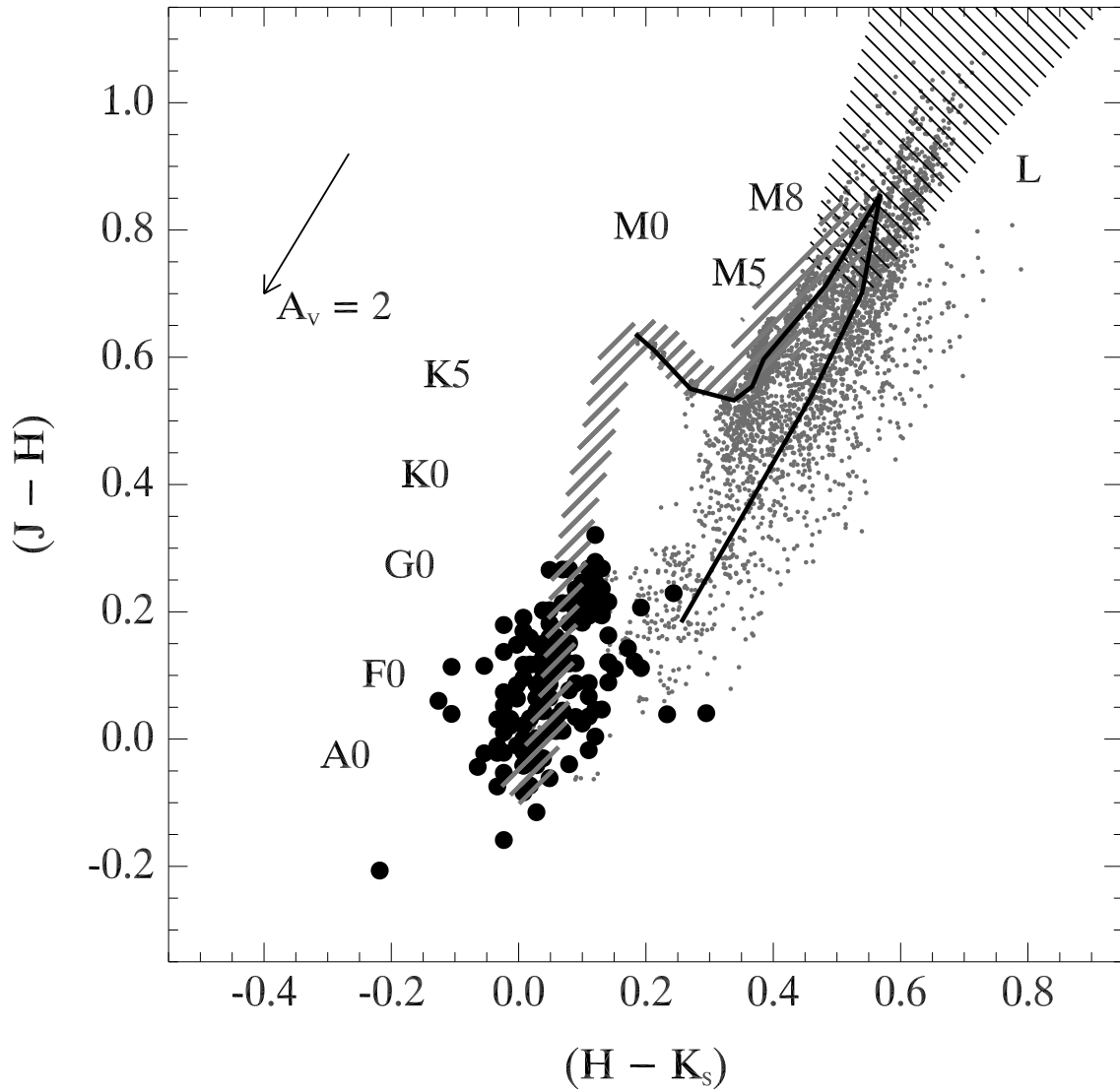


Fig. 2.— As in Figure 1, but showing the single, cool WD data from Bergeron et al. (2001) (large black circles) and simulated WD + main sequence star (M–L) binaries (small grey circles; see Section 3.2). The solid black line is a schematic representation of the displacement in the color-color diagram caused by combining a given WD with a successively later spectral type companion.

Table 1. White Dwarf + Low Mass Main Sequence Star Binary Candidates

| WD Number  | Binary?           | $J$    | $\sigma_J$ | $H$    | $\sigma_H$ | $K_s$  | $\sigma_{K_s}$ |
|------------|-------------------|--------|------------|--------|------------|--------|----------------|
| 0023+388   | MS99 <sup>a</sup> | 13.807 | 0.029      | 13.250 | 0.033      | 12.947 | 0.039          |
| 0034–211   | MS99 <sup>b</sup> | 11.431 | 0.032      | 10.911 | 0.029      | 10.636 | 0.030          |
| 0102+210.2 | MS99 <sup>c</sup> | 16.701 | 0.114      | 16.221 | 0.161      | 15.574 | 0.206          |
| 0116–231   | MS99              | 14.602 | 0.036      | 14.064 | 0.043      | 13.803 | 0.054          |
| 0130–196   | this work         | 14.785 | 0.037      | 14.270 | 0.040      | 14.023 | 0.058          |
| 0131–163   | 1                 | 12.963 | 0.035      | 12.447 | 0.033      | 12.241 | 0.034          |
| 0145–221   | this work         | 14.925 | 0.037      | 14.429 | 0.048      | 14.366 | 0.065          |
| 0148–255J  | MS99              | 12.472 | 0.026      | 11.882 | 0.034      | 11.593 | 0.029          |
| 0145–174   | this work         | 15.177 | 0.052      | 14.646 | 0.069      | 14.330 | 0.074          |
| 0205+133   | 2 <sup>d</sup>    | 12.797 | 0.030      | 12.196 | 0.029      | 11.950 | 0.025          |
| 0208–153   | this work         | 12.621 | 0.029      | 12.081 | 0.026      | 11.778 | 0.030          |
| 0219+282   | this work         | 16.067 | 0.078      | 15.587 | 0.103      | 15.293 | 0.146          |
| 0252+209   | MS99              | 16.482 | 0.110      | 16.044 | 0.147      | 16.097 | 0.322          |
| 0257–005   | this work         | 16.773 | 0.139      | 16.344 | 0.211      | 15.526 | 0.204          |
| 0303–007   | MS99              | 13.165 | 0.027      | 12.625 | 0.025      | 12.410 | 0.030          |
| 0309–275   | this work         | 13.523 | 0.034      | 12.881 | 0.030      | 12.738 | 0.033          |
| 0324+738   | MS99 <sup>e</sup> | 11.719 | 0.029      | 11.086 | 0.024      | 10.822 | 0.026          |
| 0347–137   | 1                 | 12.045 | 0.034      | 11.565 | 0.044      | 11.301 | 0.033          |
| 0355+255   | MS99 <sup>e</sup> | 9.009  | 0.046      | 8.496  | 0.041      | 8.344  | 0.028          |
| 0357+286J  | MS99              | 9.845  | 0.046      | 9.260  | 0.033      | 9.048  | 0.032          |
| 0357–233   | this work         | 15.054 | 0.048      | 14.587 | 0.058      | 14.266 | 0.073          |
| 0408+158   | MS99              | 10.777 | 0.037      | 10.199 | 0.037      | 9.926  | 0.030          |
| 0413–077   | MS99              | 6.738  | 0.019      | 6.279  | 0.041      | 5.966  | 0.047          |
| 0429+176   | MS99              | 10.755 | 0.032      | 10.115 | 0.035      | 9.927  | 0.036          |
| 0430+136   | MS99              | 13.550 | 0.033      | 12.877 | 0.039      | 12.655 | 0.041          |
| 0458–662   | MS99              | 13.431 | 0.032      | 12.686 | 0.026      | 12.511 | 0.035          |
| 0628–020   | MS99 <sup>f</sup> | 10.704 | 0.027      | 10.150 | 0.029      | 9.838  | 0.026          |
| 0752–146   | 3                 | 12.625 | 0.024      | 12.135 | 0.028      | 11.831 | 0.027          |
| 0807+190   | 4                 | 15.790 | 0.082      | 15.210 | 0.118      | 15.229 | 0.160          |
| 0812+478   | this work         | 14.578 | 0.038      | 14.149 | 0.048      | 13.849 | 0.067          |
| 0825+367   | this work         | 14.077 | 0.045      | 13.507 | 0.043      | 13.318 | 0.053          |

Table 1—Continued

| WD Number | Binary?   | $J$    | $\sigma_J$ | $H$    | $\sigma_H$ | $K_s$  | $\sigma_{K_s}$ |
|-----------|-----------|--------|------------|--------|------------|--------|----------------|
| 0851+190  | this work | 15.514 | 0.056      | 15.029 | 0.079      | 14.597 | 0.077          |
| 0904+391  | this work | 15.436 | 0.061      | 14.893 | 0.077      | 14.592 | 0.085          |
| 0908+226  | MS99      | 15.184 | 0.048      | 14.473 | 0.042      | 14.350 | 0.061          |
| 0915+201  | this work | 15.712 | 0.064      | 15.148 | 0.076      | 14.824 | 0.083          |
| 0937–095  | MS99      | 13.797 | 0.032      | 13.210 | 0.027      | 13.058 | 0.038          |
| 0950+139  | 5         | 16.430 | 0.114      | 15.555 | 0.144      | 15.350 | 0.151          |
| 0954+134  | this work | 15.561 | 0.069      | 14.838 | 0.087      | 14.548 | 0.089          |
| 1001+203  | MS99      | 12.642 | 0.040      | 12.020 | 0.032      | 11.756 | 0.037          |
| 1013–050  | MS99      | 10.635 | 0.028      | 9.985  | 0.029      | 9.775  | 0.027          |
| 1026+002  | MS99      | 11.771 | 0.032      | 11.218 | 0.032      | 10.916 | 0.027          |
| 1037+512  | this work | 13.804 | 0.031      | 13.235 | 0.028      | 12.973 | 0.029          |
| 1054+305  | MS99      | 11.888 | 0.031      | 11.168 | 0.053      | 10.982 | 0.023          |
| 1054+419  | MS99      | 9.473  | 0.032      | 8.863  | 0.031      | 8.619  | 0.033          |
| 1106+316  | this work | 15.116 | 0.048      | 14.543 | 0.053      | 14.474 | 0.102          |
| 1106–211  | this work | 14.673 | 0.040      | 13.910 | 0.047      | 13.814 | 0.058          |
| 1108+325  | this work | 15.785 | 0.072      | 15.204 | 0.084      | 15.187 | 0.181          |
| 1123+189  | MS99      | 12.777 | 0.038      | 12.232 | 0.035      | 11.999 | 0.025          |
| 1133+358  | MS99      | 11.631 | 0.036      | 11.101 | 0.054      | 10.780 | 0.037          |
| 1136+667  | MS99      | 12.369 | 0.030      | 11.749 | 0.034      | 11.615 | 0.038          |
| 1156+129  | this work | 14.702 | 0.045      | 14.104 | 0.044      | 13.885 | 0.051          |
| 1156+132  | this work | 16.886 | 0.148      | 16.224 | 0.189      | 15.939 | 0.209          |
| 1201+437  | MS99      | 15.410 | 0.050      | 14.829 | 0.061      | 13.777 | 0.043          |
| 1210+464  | MS99      | 12.076 | 0.029      | 11.414 | 0.030      | 11.167 | 0.027          |
| 1211–169  | this work | 7.945  | 0.025      | 7.340  | 0.031      | 7.190  | 0.042          |
| 1214+032  | MS99      | 9.220  | 0.030      | 8.648  | 0.030      | 8.412  | 0.027          |
| 1218+497  | this work | 14.579 | 0.041      | 13.977 | 0.042      | 13.830 | 0.063          |
| 1224+309  | 6         | 15.122 | 0.058      | 14.687 | 0.069      | 14.308 | 0.084          |
| 1229+290  | this work | 15.888 | 0.084      | 15.210 | 0.102      | 14.561 | 0.099          |
| 1236–004  | this work | 16.386 | 0.113      | 15.871 | 0.145      | 15.558 | 0.236          |
| 1247–176  | 7         | 13.536 | 0.034      | 12.892 | 0.031      | 12.601 | 0.034          |
| 1302+317  | this work | 15.837 | 0.070      | 15.295 | 0.091      | 15.113 | 0.130          |

Table 1—Continued

| WD Number | Binary?                | $J$    | $\sigma_J$ | $H$    | $\sigma_H$ | $K_s$  | $\sigma_{K_s}$ |
|-----------|------------------------|--------|------------|--------|------------|--------|----------------|
| 1307–141  | this work              | 13.869 | 0.033      | 13.229 | 0.040      | 13.019 | 0.044          |
| 1330+793  | MS99                   | 12.482 | 0.028      | 11.863 | 0.026      | 11.697 | 0.028          |
| 1333+487  | MS99                   | 11.829 | 0.024      | 11.260 | 0.027      | 10.960 | 0.033          |
| 1339+346  | this work              | 14.095 | 0.041      | 13.695 | 0.043      | 13.572 | 0.047          |
| 1412–049  | this work              | 13.726 | 0.029      | 13.107 | 0.034      | 12.975 | 0.038          |
| 1431+257  | this work              | 16.260 | 0.100      | 15.542 | 0.101      | 15.714 | 0.224          |
| 1435+370  | this work              | 13.467 | 0.030      | 12.954 | 0.039      | 12.760 | 0.032          |
| 1436–216  | this work              | 13.326 | 0.029      | 12.757 | 0.030      | 12.488 | 0.035          |
| 1443+336  | this work              | 14.265 | 0.034      | 13.697 | 0.042      | 13.509 | 0.047          |
| 1458+171  | this work              | 14.676 | 0.038      | 14.174 | 0.050      | 13.743 | 0.057          |
| 1502+349  | this work              | 15.208 | 0.050      | 14.759 | 0.071      | 14.300 | 0.072          |
| 1504+546  | 8                      | 13.854 | 0.029      | 13.250 | 0.034      | 13.003 | 0.033          |
| 1517+502  | MS99 <sup>g</sup>      | 15.553 | 0.064      | 14.744 | 0.075      | 14.133 | 0.072          |
| 1522+508  | this work              | 14.737 | 0.041      | 14.196 | 0.049      | 13.921 | 0.057          |
| 1527+450  | this work              | 16.212 | 0.090      | 15.784 | 0.117      | 15.350 | 0.205          |
| 1558+616  | MS99                   | 14.207 | 0.036      | 13.609 | 0.047      | 13.349 | 0.047          |
| 1603+125  | this work              | 13.544 | 0.033      | 13.088 | 0.036      | 12.986 | 0.031          |
| 1606+181  | this work              | 14.778 | 0.039      | 14.142 | 0.055      | 13.910 | 0.054          |
| 1610+383  | this work <sup>h</sup> | 14.404 | 0.045      | 13.750 | 0.046      | 13.560 | 0.060          |
| 1619+525  | this work              | 14.178 | 0.035      | 13.619 | 0.040      | 13.421 | 0.042          |
| 1619+414  | MS99                   | 13.918 | 0.033      | 13.272 | 0.040      | 13.009 | 0.041          |
| 1622+323  | MS99                   | 14.644 | 0.040      | 13.991 | 0.040      | 13.796 | 0.050          |
| 1631+781  | MS99                   | 10.998 | 0.031      | 10.381 | 0.031      | 10.154 | 0.026          |
| 1643+143  | 1                      | 12.766 | 0.035      | 12.096 | 0.055      | 11.955 | 0.028          |
| 1654+160  | 9                      | 13.066 | 0.045      | 12.402 | 0.059      | 12.145 | 0.042          |
| 1711+667J | 10                     | 15.088 | 0.045      | 14.430 | 0.059      | 14.213 | 0.086          |
| 1717–345  | 11                     | 12.864 | 0.027      | 12.244 | 0.052      | 12.008 | 0.046          |
| 2133+463  | MS99                   | 11.341 | 0.026      | 10.747 | 0.028      | 10.459 | 0.032          |
| 2151–015  | MS99                   | 12.478 | 0.030      | 11.787 | 0.025      | 11.443 | 0.031          |
| 2256+249  | MS99                   | 11.663 | 0.039      | 11.204 | 0.041      | 10.892 | 0.033          |
| 2317+268  | this work              | 14.614 | 0.032      | 14.067 | 0.040      | 13.769 | 0.050          |



Table 1—Continued

| WD Number | Binary?   | $J$    | $\sigma_J$ | $H$    | $\sigma_H$ | $K_s$  | $\sigma_{K_s}$ |
|-----------|-----------|--------|------------|--------|------------|--------|----------------|
| 2323+256  | this work | 15.815 | 0.077      | 15.404 | 0.133      | 15.385 | 0.164          |
| 2326–224  | this work | 12.649 | 0.028      | 12.031 | 0.039      | 11.753 | 0.030          |

References. — (1) Schultz, Zuckerman, & Becklin (1996); (2) Greenstein (1986b); (3) Schultz et al. (1993); (4) Gizis & Reid (1997); (5) Fulbright & Liebert (1993); (6) Orosz et al. (1999); (7) Koester et al. (2001); (8) Stepanian et al. (2001); (9) Zuckerman & Becklin (1992); (10) Finley, Koester, & Basri (1997); (11) Reid et al. (1988).

<sup>a</sup>WD0023+388 is a known triple system composed of a close WD + red dwarf pair with a wide red dwarf companion (Reid 1996).

<sup>b</sup>WD0034–211 is classified as a close double degenerate binary in MS99. Bragaglia et al. (1990) reclassified it as a WD + red dwarf binary, which is supported by its 2MASS colors.

<sup>c</sup>WD0102+210.2 is classified as one component of a wide double degenerate binary (Sion et al. 1991), but our 2MASS colors suggest that it may be a close WD + red dwarf binary also.

<sup>d</sup>WD0205+133 may be a sdOB + red dwarf binary, instead of a WD + red dwarf binary (Allard et al. 1994).

<sup>e</sup>This object is classified as the WD component of a wide (resolved) WD + red dwarf binary, but our 2MASS colors suggest that the WD may also be a close WD + red dwarf binary.

<sup>f</sup>The binary separation of WD0628–020 ( $4''$ ) is near the 2MASS resolution limit; there is only one entry in the 2IDR point source catalog, but these magnitudes may be for the red dwarf component only.

<sup>g</sup>The companion of WD1517+502 is a dwarf carbon star (Liebert et al. 1994).

<sup>h</sup>WD1610+383 is barely resolved on the DSS images as a common proper motion pair with red and blue components at a separation of  $\approx 4$  arcsec. Blinking of the DSS and 2MASS images suggests that only the red component is detected by 2MASS. Its near-IR colors are consistent with an early-M spectral type.

Table 2. Tentative WD + Low Mass Main Sequence Star Binary Candidates

| WD Number  | Binary?                | $J$    | $\sigma_J$ | $H$    | $\sigma_H$ | $K_s$  | $\sigma_{K_s}$ |
|------------|------------------------|--------|------------|--------|------------|--------|----------------|
| 0023–109   | MS99 <sup>a</sup>      | 16.042 | 0.081      | 15.852 | 0.172      | 15.608 | 0.237          |
| 0029–032   | this work              | 15.660 | 0.055      | 15.380 | 0.089      | 15.172 | 0.151          |
| 0518+333   | MS99 <sup>a</sup>      | 15.439 | 0.082      | 15.184 | 0.103      | 14.912 | 0.105          |
| 0710+741   | 1                      | 14.708 | 0.035      | 14.425 | 0.059      | 14.155 | 0.070          |
| 0816+387   | MS99 <sup>a</sup>      | 16.036 | 0.106      | 15.765 | 0.196      | 15.549 | 0.229          |
| 0942+236.1 | MS99 <sup>a</sup>      | 16.675 | 0.115      | 16.292 | 0.178      | 16.059 | 0.256          |
| 1008+382   | this work              | 16.883 | 0.154      | 16.646 | 0.263      | 16.290 | 0.300          |
| 1015–173   | this work              | 15.241 | 0.049      | 14.863 | 0.069      | 14.569 | 0.107          |
| 1247+550   | this work <sup>b</sup> | 15.782 | 0.071      | 15.618 | 0.135      | 15.293 | 0.469          |
| 1434+289   | this work              | 16.544 | 0.120      | 16.334 | 0.206      | 15.946 | 0.301          |
| 1639+153   | this work              | 15.065 | 0.049      | 14.960 | 0.069      | 14.595 | 0.132          |
| 2211+372   | this work              | 16.278 | 0.106      | 16.057 | 0.195      | 15.736 | 0.246          |
| 2257+162   | this work              | 15.401 | 0.062      | 15.045 | 0.074      | 14.674 | 0.110          |
| 2336–187   | this work              | 15.057 | 0.041      | 14.923 | 0.069      | 14.694 | 0.097          |
| 2349–283   | this work              | 16.119 | 0.090      | 15.863 | 0.178      | 15.549 | 0.222          |

References. — (1) Marsh & Duck (1996).

<sup>a</sup>This object is classified as the WD component of a wide (resolved) binary, but our 2MASS colors suggest that the WD may also be a close WD + red dwarf binary.

<sup>b</sup>MS99 note that WD1247+550 is “possibly the coolest known degenerate star.”